

Hybrid plasmonic waveguide in a metal V-groove

Zhao-xian Chen, Zi-jian Wu, Yang Ming, Xue-jin Zhang,^a and Yan-qing Lu^b
National Laboratory of Solid State Microstructures and College of Engineering and Applied Sciences, Nanjing University, Nanjing 210093, China

(Received 16 October 2013; accepted 16 December 2013; published online 3 January 2014)

We propose and investigate a type of hybrid plasmonic waveguide in a metal V-groove. A high-permittivity nanowire was placed in the metal channel covered with a dielectric film of lower permittivity. Deeper sub-wavelength confinement and much longer propagation distance were achieved in comparison with conventional channel plasmonic waveguides. The overall performance was improved as compared with the conventional hybrid plasmonic structure based on a flat metal surface. Finite element analysis showed that both the mode propagation and field profile can be adjusted by changing the nanowire radius and film thickness. Some benefits, such as a reduced scattering loss caused by the surface roughness, are also expected owing to the unique mode profile. The proposed approach has potential for application in high-level photonic integration. © 2014 Author(s). All article content, except where otherwise noted, is licensed under a Creative Commons Attribution 3.0 Unported License. [<http://dx.doi.org/10.1063/1.4861582>]

I. INTRODUCTION

Surface plasmon polaritons (SPP) are electromagnetic modes that exist at metal-dielectric interfaces. This phenomenon originates from oscillations between electromagnetic waves and electron plasma in the metal.^{1,2} Because the electromagnetic energy is confined to a nanometer scale in SPPs, intensive research has been conducted in recent years to explore the prospective use of SPPs in photonic integrated circuits³⁻¹¹ and nanofocusing.^{12,13} However, various plasmonic structures have both advantages and disadvantages. For example, metal films⁵ can guide long range SPP modes, but the localization is poor as the portion of the wave's energy carried in the metal is small. Metal particles⁶ can confine the field far below the diffractive limit along a chain; however, a strong attenuation is also a barrier, preventing the applications of SPPs in plasmonic interconnects. Metal wedges⁸ can strongly confine plasmonic modes to a telecommunication band, but the associated bending losses are quite large.

Among the abovementioned plasmonic structures, channel plasmon polaritons (CPPs) have been thoroughly studied, both theoretically¹⁴⁻¹⁶ and experimentally,^{3,17,18} owing to their interesting topography and strong mode confinement. If a groove is deep enough, the field of the CPP is mainly concentrated at the bottom of the metal groove. This unique property allows us to bend the CPP waveguides with a particular small curvature.¹⁹ However, the metal V-groove must be very smooth to avoid scattering loss, and it has to be very sharp to suppress the field well inside the channel. In light of the heavy scattering loss caused by the roughness of both the channel bottom and sidewalls a fine focused-ion-beam method is needed, and usually strict requirements are imposed on the fabrication precision to make a smooth metal channel.²⁰ Hybrid plasmonics (HP) was proposed recently,⁴ and it consists of a high refractive index dielectric nanowire embedded in a lower refractive index dielectric environment close to a metal surface. HP distributes the electromagnetic field both in the metal-film interface and in the high permittivity region. In turn, the HP can guide mode field in a highly confined

^axuejinzh@nju.edu.cn.

^byqlu@nju.edu.cn.

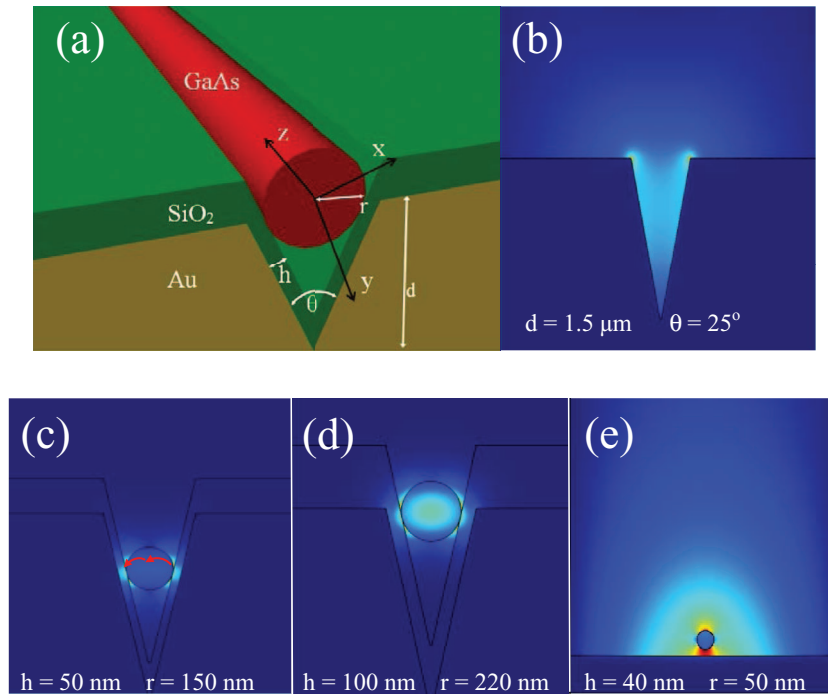


FIG. 1. (a) Schematic of a hybrid CPP waveguide consisting of a nanowire in a film-coated metal groove. Relevant parameters are denoted above. (b-d) Mode distributions of conventional CPP (b) and hybrid CPPs (c, d). Parameters are shown in the respective figures and the red arrow in (c) indicates the direction of the transverse electric field. (e) Mode distribution of a conventional hybrid plasmon with a nanowire embedded in dielectric above a flat metal surface.

mode area with relatively low propagation loss. This adjustability makes HP a powerful tool in many aspects.^{21–23} However, the mode confinement of HP is weak if the diameter of a high refractive index nanowire is too small. In this case, the high index region is not strong enough to squeeze the mode profile. In addition, in a real photonic circuit with an HP, it is not easy to manipulate and fix the nanowire at the designed position on a flat surface. Therefore, a further coating process is normally needed after the high refractive index dielectric wire is loaded on the film.⁴ As a consequence, combining the concepts of CPP and hybrid plasmonics for integrating their individual advantages is an interesting research topic. Some unique applications can also be anticipated.

In this paper, we propose a hybrid CPP based on a V-shaped groove milled in a metal film. The mode area and propagation length are numerically investigated using the Finite Element Method (FEM). By coating the metal channel with a layer of lower permittivity dielectric film and loading a higher permittivity cylindrical nanowire in it, both stronger mode confinement and weaker propagation loss are achieved. As the mode field is lifted away from the groove bottom and metal surface, the V-groove fabrication for hybrid CPP becomes less tight, and thus the difficulty in fabrication can be alleviated.²⁰ Even a rounded groove bottom is acceptable; in fact, it is desired for mass fabrication. Furthermore, the leaking mode component outside the V-groove is reduced, which significantly contributes to the minimization of the crosstalk between adjacent waveguide channels.¹⁸ Finally, we also compared the performances of our hybrid CPP with conventional HPs. Some advantages of hybrid CPPs are discussed, which are quite beneficial in high density photonic integration circuits.

II. SIMULATION AND COMPARISON

A CPP with finite channel depth, as in Fig. 1(b), can be treated as two coupled plasmonic wedges. The modes in this structure are not appreciably sub-wavelength because the mode field is not totally confined to the channel while part of the mode leaks to the outside of the V-groove. The mode width is much larger than the groove width, and the crosstalk between adjacent waveguide channels cannot

be ignored. In addition, a conventional CPP mode only propagates tens of micrometers owing to the high loss caused by the metal dissipation and groove surface scattering. To improve this, we proposed a hybrid CPP design, which is shown in Fig. 1(a). The channel is coated with a lower refractive index dielectric film supporting a high index dielectric nanowire. The wavelength considered here is $\lambda = 1550$ nm, and the metal we use is gold with a permittivity $\epsilon_{\text{gold}} = -132 + 12.65i$.²⁴ The opening angle θ of the metal channel is 25° , which is a commonly adopted parameter for CPPs. The depth of the channel is $d = 1.5$ μm . The material of choice for the film is SiO_2 with a permittivity of $\epsilon_{\text{silica}} = 2.25$, and its thickness is h . The nanowire has a radius r , and it consists of GaAs, which has a much higher permittivity $\epsilon_{\text{GaAs}} = 12.25$. To mimic the real case, we also assume that all the corners that appear in this structure are rounded with a rounding radius $r_0 = 10$ nm. All these components are exposed to air and the Cartesian coordinate axes used for the analysis are also shown. The y axis is parallel to one sidewall of the groove and the propagation is along the z -axis direction.

We analyze the proposed tunable hybrid CPP modes according to the simulation results. In Fig. 1, on comparing the panels (c-d) with (b), the mode confinement in the proposed hybrid CPP is observed to be much stronger than that in conventional CPPs. The hybrid mode still exhibits some characteristics of the CPP because its transverse electric field component, the red arrow in Fig. 1(c), is perpendicular to the surface of the metal groove. Because the hybrid mode mainly lies in the upper part of the groove, many unique and useful properties emerge. For example, the balance between the mode confinement and propagation length is now easily adjustable for the hybrid mode. The mode area could be greatly reduced with negligible field outside of the channel. As a result, the crosstalk and coupling with other adjacent waveguides are diminished, which is of great importance in highly integrated optical circuits.¹⁸ Besides, scattering loss caused by the roughness of the channel's bottom and sidewalls also decreases as the mode intensity on the metal surface is reduced. Comparing Fig. 1(c)–1(d) with Fig. 1(e) also reveals the advantages of a hybrid CPP over a conventional HP; the confinement of the hybrid CPP is better, especially when the high refractive index region is small. Since there is a V-groove machined on the metal film, it would be much easier to incorporate the nanowire into it to form a hybrid CPP. The metal groove could thus hold the nanowire precisely and tightly even if there is no further process to fix the structure. Because the nanowire is not fixed, it can be replaced if another wire should be used for some purpose. From this point of view, although the fabrication of the V-groove requires fine machining, the resulting system can be conveniently reconfigured in the subsequent plasmonic waveguide fabrication and device applications. Significant attention is now devoted to studying the luminescence properties of various nanowires. Thus, nanowire loading may even lead to future active hybrid CPP applications, and it can constitute a viable solution for loss reduction in plasmonic devices. We believe the proposed hybrid approach is likely to be very promising in improving the performances of conventional CPPs.

III. SIMULATION RESULTS AND DISCUSSION

In order to arrive at a full understanding of this hybrid CPP, the effective index, mode area and propagation distance of this plasmonic waveguide were thoroughly studied. Comparison with the conventional CPP and HP is also presented in what follows, along with the discussion of results.

Because the hybrid mode field is distributed both in the cylindrical nanowire and in the SiO_2 film, the hybrid CPP can be regarded as the hybridization of the film-coated CPP (without the nanowire in the hybrid CPP) and the dielectric waveguide mode (DWM, without the metal component in the hybrid CPP). As a consequence, a hybrid CPP could be divided into the film-coated CPP-like component (with field localized mainly in the film) and the DWM-like component (with field localized mainly in the cylindrical wire). Figure 2(a) shows the effective index of the hybrid CPP as a function of h and r . It is apparent that the effective index has a much stronger dependence on r than on h . For a given film thickness, changing the nanowire radius greatly affects the effective index. In contrast, changing the film thickness makes less difference when the radius is fixed. As shown by the blue dashed curve in Fig. 2(b), the DWM's mode index changes significantly when the nanowire radius is larger than 140 nm, below which the mode is cut off. However, the film-coated CPP's effective index only changes from 1.02 to 1.35 when the film thickness ranges from 10 nm to 100 nm. The red solid and dashed curves in Fig. 2(b) show the effective indices of the hybrid CPP

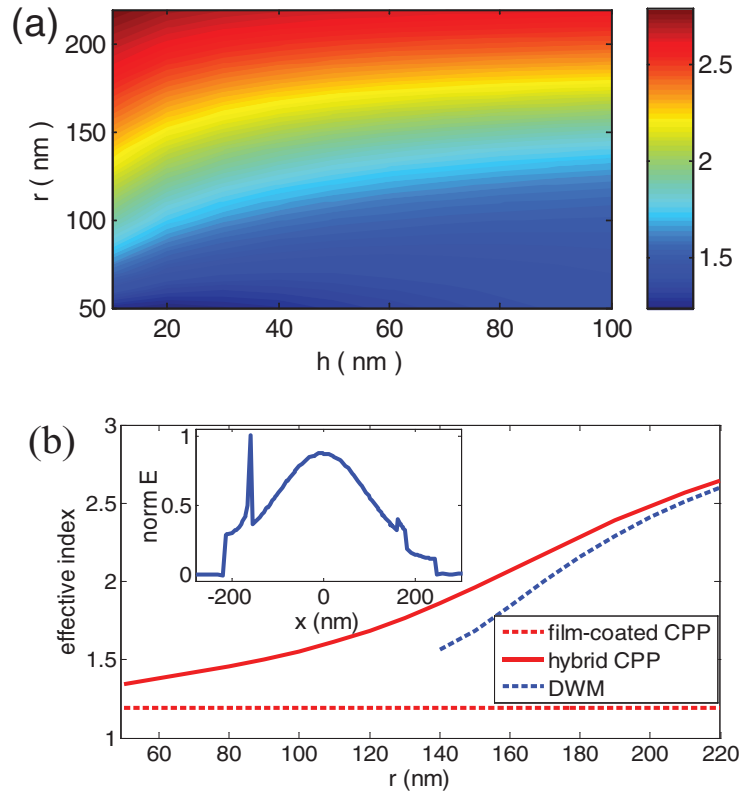


FIG. 2. (a) The effective index of the hybrid CPP as a function of r and h . (b) Dispersion relations of the DWM (blue dashed curve) and hybrid CPP with $h = 60$ nm (red solid curve). The red dashed line indicates the effective index of the film-coated CPP with $h = 60$ nm. Inset shows the normalized electric field of the hybrid CPP along the x axis with $r = 160$ nm and $h = 60$ nm.

and film-coated CPP, respectively, when the film thickness is $h = 60$ nm. For increasing nanowire radii, the hybrid CPP's effective index shifts closer to the DWM's index but further away from the film-coated CPP's index. This leads to an increase of the DWM-like component and a decrease of the film-coated CPP-like component in the hybrid CPP. The inset in Fig. 2(b) shows the hybrid CPP's normalized electric field along the x axis, which is perpendicular to one of the metal groove's surfaces. The origin of the coordinate system is located at the center of the nanowire. The hybrid CPP we study here has $h = 60$ nm and $r = 160$ nm. The steep slope on the left side of the curve represents high field contrast between the metal's inside and SiO₂ film. The highest peak on the film/nanowire boundary reveals that the field is attracted toward the high-index region, which is a typical feature of hybrid plasmonic mode. The electric field's exponential damping in the dielectric film testifies the weak dependence of the effective index on the film thickness. On the other hand, the peak at $x = 0$ implies the presence of a strong electric field inside the nanowire, which is quite different from what was reported in a previous work.⁴ A major portion of the light intensity is drawn from the film to the nanowire, causing the hybrid mode's strong dependence on the nanowire's radius.

We analyze the mode area, as defined in Ref. 25, which clearly reflects the total energy localization,

$$A_m = \min_{f(r)} \int_{A_\infty} f(r) dA, \quad s.t. \quad \int_{A_\infty} [f(r) - \eta] W(r) dA = 0 \quad (1)$$

In Equation (1), $W(r)$ is the electromagnetic energy density and $f(r)$ is a shape function that encompasses a fraction η of the mode's energy density. For simplification, we consider $\eta = 0.5$ and treat $f(r)$ as a step function bounded by a constant energy density contour W_0 , $f(r) = 0$, if $W(r) < W_0$ and $f(r) = 1$, if $W(r) > W_0$. The mode area is normalized by $A_0 = 3.20E-13m^2$, which is

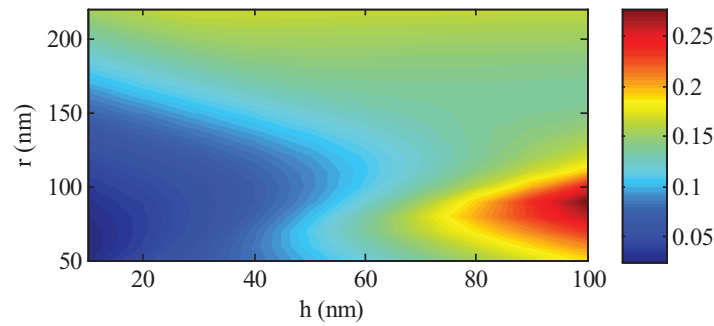


FIG. 3. Normalized mode area of the hybrid mode, A_m/A_0 , as a function of r and h .

the mode area of the conventional CPP in Fig. 1(b), obtained by solving the same equation. The variation tendency with respect to the normalized mode area, A_m/A_0 , of this hybrid CPP is derived by analyzing Fig. 3. First, the hybrid CPP's mode area is significantly reduced as compared with the area of the conventional CPP. In addition, the hybrid CPP with the smallest r and h has the minimal area, and an increase in mode area for increasing film thickness is apparent for $r < 180$ nm. This tendency could be attributed to the increase of the film-coated CPP's portion in the hybrid CPP. However, this tendency disappears for $r \geq 180$ nm because the hybrid mode's area does not show an obvious increase with increasing film thickness. The nanowire is gradually lifted out of the metal channel when the film is thickened, and the DWM-like component assumes a major portion of the hybrid CPP. Consequently, thickening the film makes little difference because a major portion of the mode has been constrained inside the nanowire. In fact, hybrid CPPs with large wires and thick films act as a dielectric waveguide system because the plasmonic property is insignificant. These extreme cases were included in our parametric analysis because they provide us with the information regarding the selection of parameters for designing a hybrid mode. Another interesting phenomenon is that the largest mode area occurs when $r = 90$ nm and $h = 100$ nm. With a small wire and thick film, the film-coated CPP component occupies a major portion in the hybrid CPP as most of the mode field is distributed in the thick film, which leads to a large mode area. With increasing radius, the wire attracts the mode field in and around it. In turn, the mode area decreases although the light intensity inside the nanowire becomes large. In fact, if we extend the parametric range to smaller r and h , the mode area exhibits a reverse change for $r < 50$. Hybrid CPP cannot be well-formed if the nanowire diameter is too small and the mode leakage is very large. The normalized mode area exhibits an abrupt increase when the radius of the nanowire is smaller than 50 nm and finally reaches 1 for $h = 0$ and $r = 0$.

In addition to the mode area, the propagation length is another key feature of a hybrid CPP, and its value can be obtained from the following formula,

$$L = \frac{1}{2\text{Im}[\beta(h, r)]}. \quad (2)$$

This is a general formula, where $\beta(h, r)$ is the mode's complex wave vector. The results are shown in Fig. 4. Conversely, a conventional CPP, with its corresponding mode profile shown in Fig. 1(b), only travels approximately $44 \mu\text{m}$, as shown by the red contour in Fig. 4. It is clear that the zone above the red curve corresponds to hybrid CPPs, the propagation lengths of which are longer than those of conventional CPPs. Length extension of 1–2 orders of magnitude is achievable. Enlarging the nanowire radius increases the DWM-like component of the hybrid CPP while thickening the film decreases the mode's portion in the metal. All these tendencies account for weaker SPP confinement and longer propagation distance. In a real device design, there should be a trade-off between the mode confinement and propagation length.

Further, we compared the overall performances of the hybrid CPP and the conventional HP. Figure of merit (FOM) is defined as the ratio between the propagation length and mode area.^{4,26} FOM may reflect the quality of a structure, and a high FOM is desired. A direct comparison of FOMs is given in Fig. 5, where the color bar reflects the ratio between the FOMs of hybrid CPP

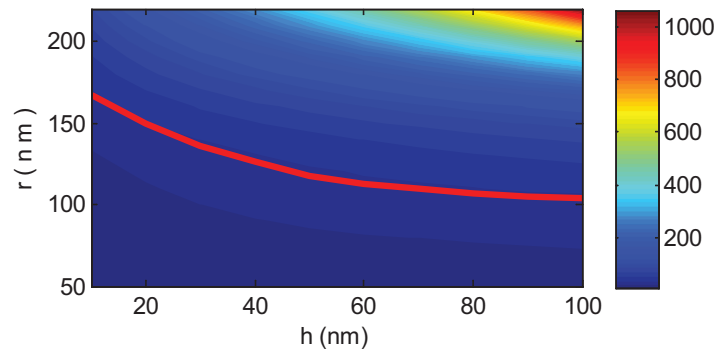


FIG. 4. Propagation length of a hybrid CPP, in units of μm . The red solid curve corresponds to a conventional CPP with a propagation distance of $44 \mu\text{m}$.

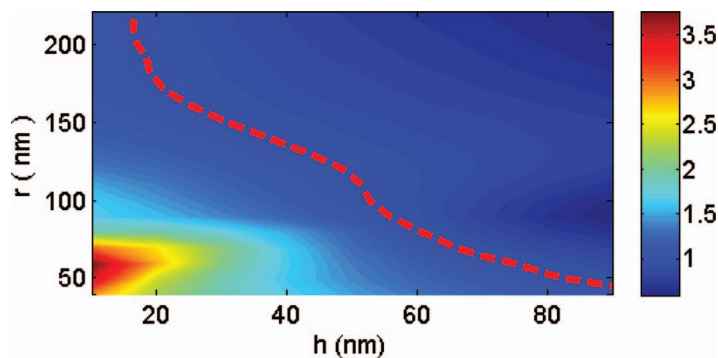


FIG. 5. The ratio between the FOMs of hybrid CPP and conventional hybrid plasmonic waveguide. The red dashed curve corresponds to 1, implying that hybrid CPP and conventional hybrid plasmonic waveguide have the same FOM.

and conventional HP. The red dashed line corresponds to 1 and the part in Fig. 5 below the curve indicates that a hybrid CPP performs better than a conventional HP. Figure 1(e) is the mode profile of the conventional HP with a nanowire that has a radius $r = 50 \text{ nm}$ and is located 40 nm away from the metal surface. It is apparent that when a smaller nanowire is adopted, a hybrid CPP yields a larger FOM, which is much preferred for a waveguide.

IV. CONCLUSIONS

We proposed and investigated a hybrid plasmonic waveguide based on a metal channel. Some unique hybrid modes are formed as the original lossy CPP mode is lifted up owing to the nanowire loaded inside the film-coated metal groove. The mode characteristics of hybrid CPPs have been extensively investigated through FEM simulations. The hybrid CPP shows much better performance than conventional CPP and HP. The mode profiles are easily adjustable according to the agile tunable parameters. All these merits are of great interest for developing future plasmonic and photonic circuits.

ACKNOWLEDGMENTS

This work is sponsored by “973” programs 2011CBA00200 and 2010CB327803, and the NSFC programs 61225026 and 11274159. We also thank the support from PAPD. All correspondence related to this article should be addressed to Dr. Yan-qing Lu or Dr. Xue-jin Zhang.

¹ S. A. Maier, *Plasmonics: Fundamentals and Applications* (Springer, 2007), Chap. 2.

² A. Liebsch, *Phys. Rev. Lett.* **54**, 67–70 (1985).

³ S. I. Bozhevolnyi, V. S. Volkov, E. Devaux, J.-Y. Laluet, and T. W. Ebbesen, *Nature (London)* **440**, 508–511 (2006).

- ⁴R. F. Oulton, V. J. Sorger, D. A. Genov, D. F. P. Pile, and X. Zhang, *Nat. Photon.* **2**, 496–500 (2008).
- ⁵Z. J. Wu, X. K. Hu, Z. Y. Yu, W. Hu, F. Xu, and Y. Q. Lu, *Phys. Rev. B* **82**, 155107 (2010).
- ⁶S. A. Maier, P. G. Kik, H. A. Atwater, S. Meltzer, E. Harel, B. E. Koel, and A. A. G. Requicha, *Nat. Mater.* **2**, 229–232 (2003).
- ⁷G. Veronis and S. Fan, *Opt. Lett.* **30**, 3359–3361 (2005).
- ⁸D. F. P. Pile, T. Ogawa, D. K. Gramotnev, T. Okamoto, M. Haraguchi, M. Fukui, and S. Matsuo, *Appl. Phys. Lett.* **87**, 061106–061103 (2005).
- ⁹Y. Ming, Z. J. Wu, H. Wu, F. Xu, and Y. Q. Lu, *IEEE Photonics J.* **4**, 291–299 (2012).
- ¹⁰X. Zhang, H. Tang, J. A. Huang, L. Luo, J. A. Zapien, and S.-T. Lee, *Nano Lett.* **11**, 4626–4630 (2011).
- ¹¹Z. J. Wu, Y. Ming, F. Xu, and Y. Q. Lu, *Opt. Express* **20**, 17192–17200 (2012).
- ¹²M. I. Stockman, *Phys. Rev. Lett.* **93**, 137404 (2004).
- ¹³H. Choo, M.-K. Kim, M. Staffaroni, T. J. Seok, J. Bokor, S. Cabrini, P. J. Schuck, M. C. Wu, and E. Yablonovitch, *Nat. Photon.* **6**, 838–844 (2012).
- ¹⁴D. F. P. Pile and D. K. Gramotnev, *Opt. Lett.* **29**, 1069–1071 (2004).
- ¹⁵K. C. Vernon, D. K. Gramotnev, and D. F. P. Pile, *J. Appl. Phys.* **103**, 034304–034306 (2008).
- ¹⁶E. Moreno, F. J. Garcia-Vidal, S. G. Rodrigo, L. Martín-Moreno, and S. I. Bozhevolnyi, *Opt. Lett.* **31**, 3447–3449 (2006).
- ¹⁷V. S. Volkov, S. I. Bozhevolnyi, S. G. Rodrigo, L. Martín-Moreno, F. J. García-Vidal, E. Devaux, and T. W. Ebbesen, *Nano Lett.* **9**, 1278–1282 (2009).
- ¹⁸V. A. Zenin, V. S. Volkov, Z. Han, S. I. Bozhevolnyi, E. Devaux, and T. W. Ebbesen, *Opt. Express* **20**, 6124–6134 (2012).
- ¹⁹V. S. Volkov, S. I. Bozhevolnyi, E. Devaux, and T. W. Ebbesen, *Appl. Phys. Lett.* **89**, 143108–143103 (2006).
- ²⁰S. I. Bozhevolnyi, V. S. Volkov, E. Devaux, and T. W. Ebbesen, *Phys. Rev. Lett.* **95**, 046802 (2005).
- ²¹R. F. Oulton, V. J. Sorger, T. Zentgraf, R.-M. Ma, C. Gladden, L. Dai, G. Bartal, and X. Zhang, *Nature (London)* **461**, 629–632 (2009).
- ²²F. F. Lu, T. Li, J. Xu, Z. D. Xie, L. Li, S. N. Zhu, and Y. Y. Zhu, *Opt. Express* **19**, 2858–2865 (2011).
- ²³X. Yang, Y. Liu, R. F. Oulton, X. Yin, and X. Zhang, *Nano Lett.* **11**, 321–328 (2011).
- ²⁴E. D. Palik, *Handbook of Optical Constants of Solids* (Academic Press, 1985).
- ²⁵R. F. Oulton, G. Bartal, D. F. P. Pile, and X. Zhang, *New J. Phys.* **10**, 105018 (2008).
- ²⁶R. Buckley and P. Berini, *Opt. Express* **15**, 12174–12182 (2007).